Magnetization reversal in $Fe_{48}Pt_{34}B_{18}$ magnetic foils*

Gao You-Hui(高有辉)†

Department of Physics, Beijing Normal University, Beijing 100875, *China*

(Received 18 April 2011; revised manuscript received 17 May 2011)

Exchange-spring magnet L1-FePt/(Fe_2B+α-Fe) is fabricated by flash annealing a melt-spun $Fe_{48}Pt_{34}B_{18}$ foil. A coercivity of 8500 Oe (1 Oe = 79.5775 A/m), squareness (M_r/M_s) of 0.70, saturation magnetization of 10.2 kGs (1 Gs = 10^{-4} T) and an effective anisotropy $K_{eff} = 2.0 \times 10^7$ ergs/cm^3 are obtained. A two-step magnetization reversal feature is characterized in this paper. An exchange bias phenomenon is also observed in a low saturation field.

Keywords: L1-FePt, melt-spun, magnetic exchange interaction

PACS: 75.50.Tt, 75.60.Ej **DOI:** 10.1088/1674-1056/20/10/107502

1. Introduction

Exchange-spring magnets[1] (ESMs) have been studied for decades since the seminal work was reported by Coehoorn *et al.*,[2] in which a melt-spun $Nd_{4.5}Fe_{77}B_{18.5}$ alloy showed desirable hard magnetic properties although it contained an 85% volume ratio of magnetically soft phases (Fe_3B and α-Fe). Such magnets possessed much higher remanence and lower cost than those of their single-phase counterparts, and were expected to make a breakthrough in the enhancement of the energy product, $(BH)_{max}$. However, the obtained $(BH)_{max}$ was still significantly lower than that predicted by theory[3] in spite of a huge obtainable isotropic remanence ratio. The main reason was considered to be that the proposed heterostructures[1] (uniformly dispersed, crystallographically coherent, and well-oriented ferromagnetic nanograins) were impossible to be produced by melt-spinning,[2,4,5−7] mechanical milling,[8−10] sputtering,[11−13] and even self-assembling techniques[14,15] which could control constituents at the nanometer scale.

The magnetic properties, related to the unique magnetization progresses in ESM, strongly depend on the complicated microstructure. According to micromagnetism theory,[16] the total free energy of ESM is given as follows:

$$E_{tot} = \int \left[A(\text{grad}\, \boldsymbol{m})^2 + E_{an}(\boldsymbol{m}) - \boldsymbol{H}_{ex} \cdot \boldsymbol{J} - \frac{1}{2}\boldsymbol{H}_d \cdot \boldsymbol{J} \right] \mathrm{d}V. \quad (1)$$

Here, $A(\text{grad}\, \boldsymbol{m})^2$, E_{an}, $-\boldsymbol{H}_{ex} \cdot \boldsymbol{J}$, and $-\boldsymbol{H}_d \cdot \boldsymbol{J}/2$ are the exchange, the anisotropy, the external field, and the stray field energies, respectively; $\boldsymbol{m}$ is the unit vector of the magnetization vector $\boldsymbol{J} = J_s\boldsymbol{m}$. Note that the magnetoelastic energy is neglected in the above equation. Minimum energy should correspond to a metastable magnetic state at an applied field $\boldsymbol{H}_{ex}$. The anisotropy energy E_{an} includes all the energies contributed from crystal and structural magnetic anisotropies. Especially, the structural part, including the interface anisotropy originated in the reduced symmetry of the atomic environment around the grain boundary and the exchange anisotropy due to the exchange coupling between hard and soft magnetic phases, results in hardness of the soft phase. On the other hand, the stray field energy $-\boldsymbol{H}_d \cdot \boldsymbol{J}/2$ caused by spatial fluctuation of the compositions and discontinuity of magnetization at grain boundaries gives rise to a very complicated magnetic structure. Based on the theory, dependence of reversal field on the soft phase thickness was discussed with an oriented nanostructure,[17,18] i.e., the reversal filed was identical with the nucleation field of the hard phase for soft phase thickness thinner than the hard magnetic Bloch wall width, and then decreased rapidly with the further increase of the soft phase thickness (decreasing with the soft phase thickness to –1.75 power). It was shown that the dimension of the soft phase was the most important factor in the sense of its influence on magnetic property. However, this model was not able to figure out the magnetization rever-

*Project supported by the Foundation for Key Program of Ministry of Education, China (Grant No. 109025) and the Fundamental Research Funds for the Central Universities of China (Grant No. 101-105113).

†Corresponding author. E-mail: ygao@bnu.edu.cn

© 2011 Chinese Physical Society and IOP Publishing Ltd

sal mechanism. In a practical ESM the strong intergranular exchange interaction results in a magnetic vortex structure[19] to dramatically reduce the stray field energy. This nonuniform magnetic structure incurs the switch of the hard phase magnetization at much lower field than Bloch wall movement. The low coercivity was proved to be attributed to this nature in strong exchange-coupling systems—both multiple-phase and single-phase. Here, magnetic properties of an L1-FePt/(Fe_2B+α-Fe) nanocomposite are studied in order to obtain an insight into magnetization reversal process appearing in ESM. We choose such a system because the ordered face-centred tetragonal (FCT) FePt phase indicates extremely large magnetocrystalline anisotropy ($\sim 7\times10^7$ ergs/cm^3) so that there is a large field range for observing magnetization evolution in the soft phase before the hard phase switching.

2. Experiment

Ingot of FePtB, using metals of Pt with a purity of 99.95% and FeB alloy (B 13 wt%) balanced with electrolytic iron, was prepared by arc melting several times to obtain a homogeneous composition and melt spun at a wheel speed of 30 m/s in an argon atmosphere. The as-spun foils were subsequently flash-annealed at 823 K for 10 min under argon protection. The stoichiometric composition was evaluated to be about $Fe_{48}Pt_{34}B_{18}$ by energy-dispersive spectroscopy. The X-ray diffraction pattern indicated that the sample was constituted of L1-FePt, Fe_2B and α-Fe phases. Microstructure was observed by transmission electron microscopy (TEM). Domain structure was studied by magnetic force microscopy (MFM). The hysteresis loop was measured with superconducting quantum interference device (SQUID).

3. Results and discussion

Figure 1 shows the bright field TEM image (Fig. 1(a)) and the high resolution TEM image (Fig. 1(b)) of a grain with white contrast. It is found that the FePt gains (white contrast) display truncated polyhedra with sharp edges and are randomly dispersed in a gray matrix (Fe_2B+α-Fe). The mean grain size counted with Digital Micrograph is about 60 nm, but a large size distribution is clearly observed. The crystal structure can be confirmed by the electron diffraction pattern (see the inset of Fig. 1(a)) to be chemically ordered face-centered tetragonal (FCT) phase with a space group of $P4/mmm$ and lattice parameters of $a \approx 0.385$ nm, and $c \approx 0.371$ nm. The high resolution TEM image shows that each FePt grain has a single crystal structure.

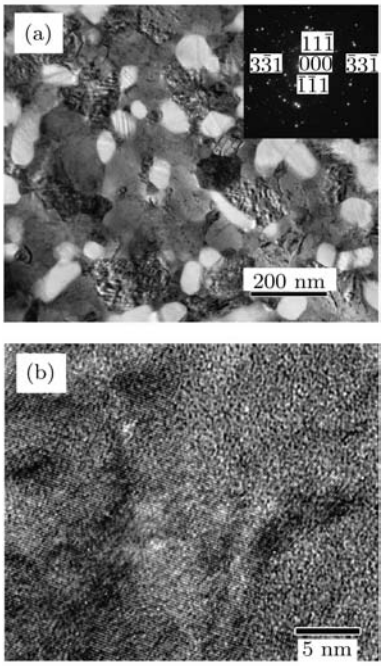


Fig. 1. Bright field TEM image (a) and the high resolution TEM image (b) of a grain with white contrast. The inset shows the crystal structure that can be confirmed by the electron diffraction pattern from a white contrast grain.

Domain structures were investigated by MFM at room temperature in air, using the tapping/lift^{TM} mode with a magnetic tip of microfabricated Si cantilever coated by CoCr layer (several tens of nanometers in thickness). The tip scanning height for MFM recording was maintained at 100 nm. Figures 2(a) and 2(b) are the MFM images recorded on the free side and the wheel side of the foil, respectively. The magnetic structures can be characterized by spike domains, which are always formed in magnetic heterostructures with huge magnetocrystalline anisotropy due to the compromise between demagnetization energy and domain wall energy. The domain size ($\sim$300 nm) is much bigger than the grain size, indicating a strong intergranular exchange coupling. It is also found that the domains on the free side are larger than those on the wheel side. We attribute it to the grain size difference between both sides resulting from the variation of cooling rate in the melt spinning process.

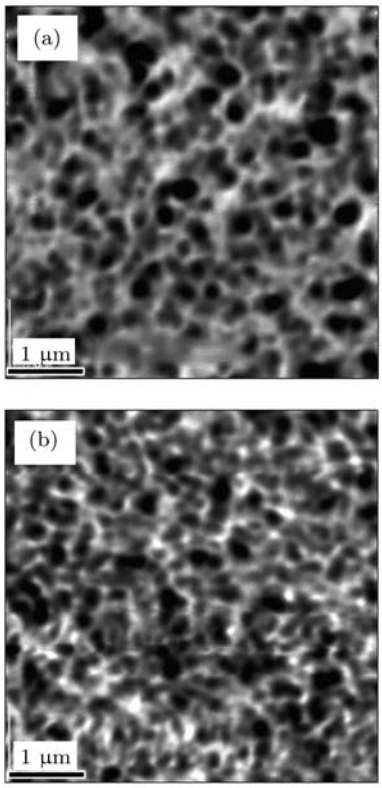


Fig. 2. MFM images recorded on the free side (a) and the wheel side (b) of the foil, showing spike domain structure. The domain size is about 300 nm.

Figure 3(a) shows the hysteresis loop measured by applying a field in the foil plane using SQUID at 300 K. A coercivity of 8500 Oe (1 Oe = 79.5775 A/m) is observed and squareness (M_r/M_s) is estimated at 0.70, much higher than the Stoner–Wohlfarth limitation (0.50) for isotropic magnetic materials. The saturation magnetization can be calculated to be 10.2 kGs (1 Gs = 10^{-4} T) by the law of approach to saturation from the initial magnetization curve of the sample saturated up to 70 kOe. The effective anisotropy $K_{\rm eff} = 2.0 \times 10^7$ ergs/cm^3 is then obtained from the fitting coefficient of $1/H^2$. It indicates that the FePtB foil has very good hard magnetic property. The magnetization variation as a function of time is recorded under a reversal field of 5 kOe for the foil saturated at 70 kOe as shown in Fig. 3(b). Although the phenomenon of magnetic viscosity in exchange coupling system is still a question to be answered, the logarithmic time decay of magnetization is still observed in our sample. Such a time dependence, which arises from thermal agitation of magnetic moments over energy barrier with a broad distribution, demonstrates that lots of structural defects in the foil, such as the grain size nonuniformity, the spatial distribution inhomogeneity of the L1-FePt phase, some interface defects, etc., induce a fluctuation of intergranular exchange interaction, resulting in a wide distribution of switching fields. Note that the magnetization hops around the fitting curve (ranging from 0 to 1000 s) reflect a balance between the thermal agitation and the magnetic interaction from neighbour grains, which are always observed in ESM systems.

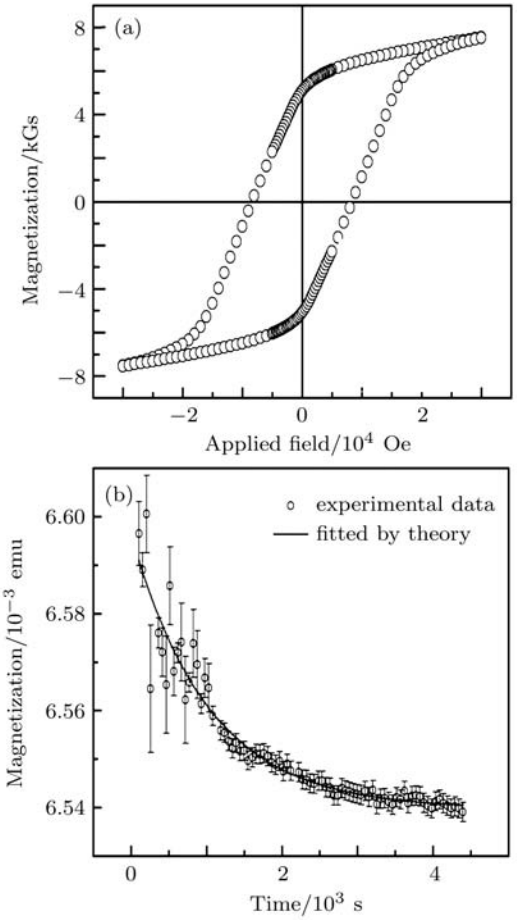


Fig. 3. (a) Hysteresis loop measured with applied field in the foil plane at 300 K, (b) the magnetization variation as a function of time recorded under a reversal field of 5 kOe for the foil saturated at 70 kOe. The experimental data are fitted by the function of $M(t,H) = M(0,H)[1 - S(H)\ln(t)]$.

A foil with initial magnetic state was saturated successively from 1 kOe to 30 kOe. A series of loops was recorded as shown in Fig. 4. It is found that the loops are asymmetric at low saturation fields as seen in Figs. 4(a)–4(c), ΔH = 129 Oe and 571 Oe at the saturation field of 1 kOe and 6 kOe, respectively. The loop displacement to the negative field is enhanced with H_s increasing up to about 10 kOe and then drops off till H_s is over 30 kOe (Fig. 4(d)). The saturation remanence M_r^+ is larger than the reverse saturation remanence M_r^- under a low saturation field at which magnetization rotation of the hard grain does not take

place yet, indicating part of soft magnetic moment is irreversible due to the pinning effect of the hard grains. The difference $\Delta M_{\rm r} = M_{\rm r}^{+} - M_{\rm r}^{-}$ produces an inner effective field along the direction of the saturation field and results in a loop displacement. Such exchange-bias behaviours just indicate the strong exchange interaction between high anisotropy phase L1-FePt and the soft phase (Fe_2B+α-Fe). A "shoulder" on the demagnetization curve of $H_{\rm s}$ = 6 kOe as arrowed in the figure, shows a two-step magnetization reversal feature in the whole demagnetization process, which can be explicitly distinguished in curves of $\mathrm{d}M/\mathrm{d}H$ against H as shown in Fig. 4(f). The curves with $H_{\rm s} > 7$ kOe indicate two cusps at around –880 Oe ($H_{\rm s}$ = 1 kOe) and –7 kOe corresponding to the switching of the soft phase and the hard phase, respectively. It is worth while noting that the first cusp becomes smaller and shifts to the high field with $H_{\rm s}$ increasing from –880 Oe for $H_{\rm s}$ = 1 kOe to –3000 Oe for $H_{\rm s}$ = 30 kOe. The high saturation field seems to induce a much more collective magnetization reversal than the low field does.

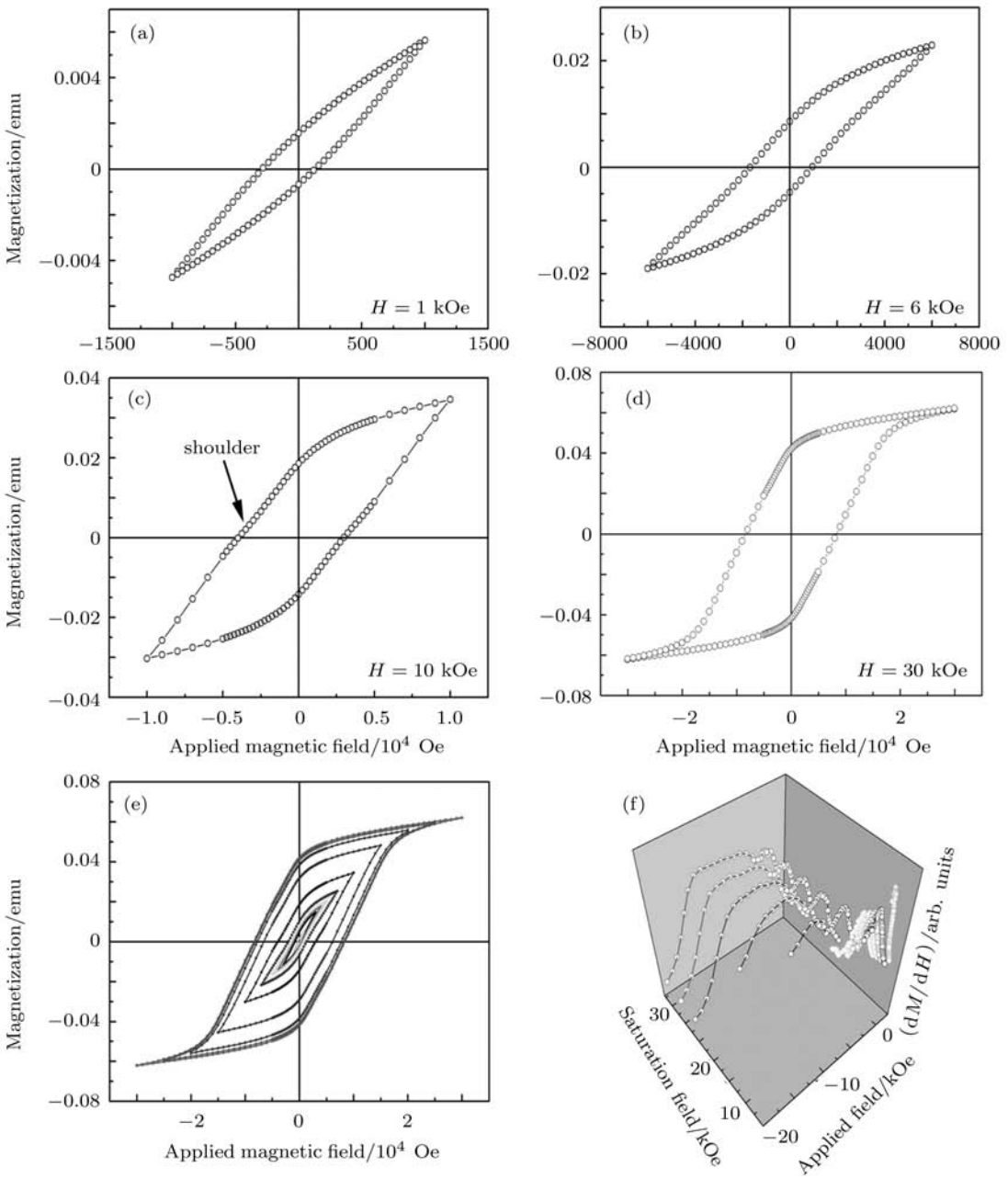


Fig. 4. Hysteresis loops obtained with saturation magnetic fields of 1 kOe (a), 6 kOe (b), 10 kOe (c), and 30 kOe (d), (e) a series of loops successively recorded for a foil with different saturation fields from 1 kOe to 30 kOe, and (f) curves of $\mathrm{d}M/\mathrm{d}H$ against H showing two cusps corresponding to the switching of the soft phase and the hard phase.

Dependence of the exchange-bias field, $H_{\rm E}$, on saturation field is plotted in Fig. 5(a). Corresponding to the two magnetization reversal processes mentioned above, $H_{\rm E}$ shows two tendencies with the saturation field. For $H_{\rm s} < 7$ kOe where only the soft phase reversal takes place, $H_{\rm E}$ increases with saturation field increasing, i.e., the more soft phase take part in the magnetization reversal process with a high applied field, the larger will the irreversible magnetization $\Delta M_{\rm r}$ pinned by the L1-FePt matrix be. However, such an L1-FePt scaffolding collapses due to the fact that some hard grains switch in the high field over 7 kOe. The reversed L1-FePt grains induce magnetization overturn of the neighbour soft grains and thereby reduce $\Delta M_{\rm r}$. So, a downward tendency of $H_{\rm E}$ with the saturation field is observed when $H_{\rm s} > 7$ kOe. The linear dependence of $H_{\rm E}$ on $H_{\rm s}$ infers a broad distribution of switching field of the hard phase, which is in good agreement with the magnetic viscosity result. After the foil was saturated at 70 kOe, a dc field H in the opposite direction was subsequently applied and the dc demagnetization remanence $M_{\rm d}(H)$ was recorded to describe the irreversible magnetization change induced mainly by the hard phase switching. Figure 5(b) shows the plot of $[M_{\rm r} - M_{\rm d}(H)]/2M_{\rm r}$ versus H. A linear dependence of $[M_{\rm r} - M_{\rm d}(H)]/2M_{\rm r}$ on H is observed at low applied fields, while the irreversible remenance reaches a saturation value when H is over 30 kOe after a rapid increase. It also infers two different reversal processes involed. The experimental data are fitted by the theoretical curve $\sin\theta$ versus $H_{\rm no}/\cos\theta$ according to the Kondorskij model[20] of completely inhomogeneous rotation, where $H_{\rm no}$ is the critical field for irreversible magnetization reversal of the hard grains, θ is the angle between the magnetic field and the easy axis. $H_{\rm no} = 9.8$ kOe is then obtained. According to Ref. [1], the critical field $H_{\rm no}$ for an isotropic system is given as follows:

$$H_{\rm no} \approx \frac{K_{\rm eff}}{\mu_0 M_{\rm s}}. \tag{2}$$

The effective anisotropic constant $K_{\rm eff}$ is estimated to be 1.12×10^7 ergs/cm^3, which is slightly smaller than that estimated by the law of approach to saturation. This deviation may results from the approximation of the model.

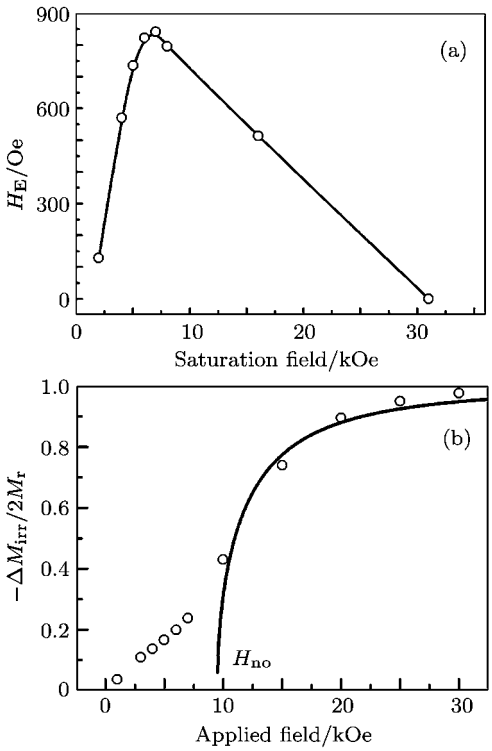


Fig. 5. (a) Dependence of the exchange-bias field on saturation field, and (b) the plot of $[M_{\rm r} - M_{\rm d}(H)]/2M_{\rm r} = -\Delta M_{\rm irr}/2M_{\rm r}$ versus H. The experimental data are fitted by the theoretical curve $\sin\theta$ versus $H_{\rm no}/\cos\theta$. $H_{\rm no} = 9.8$ kOe is obtained.

In conclusion, exchange interaction between the L1-FePt matrix and the (Fe_2B+α-Fe) soft phase in $Fe_{48}Pt_{34}B_{18}$ foil results in two magnetization reversal processes, one is only the soft phase reversal taking place in an external field below 7 kOe and another one involves hard grains switching in a high field. A coercivity of 8500 Oe squareness ($M_{\rm r}/M_{\rm s}$) of 0.70, saturation magnetization of 10.2 kGs, and an effective anisotropy $K_{\rm eff} = 2.0 \times 10^7$ ergs/cm^3 is obtained. An exchange bias phenomenon is observed due to the irreversible magnetization change of the soft phase magnetic moment in the demagnetization process.

References

[1] Kneller E F and Hawig R 1991 *IEEE Trans. Mag.* **27** 3588

[2] Coehoorn R, de Mooji D B, Duchateau J P W B and Buschow K H J 1988 *J. Phys.* (Paris) C **8** 669

[3] Skomski R and Coey J M D 1993 *Phys. Rev.* B **48** 15812

[4] Gao Y, Zhu J, Weng Y, Park E B and Yang C J 1998 *J. Appl. Phys.* **84** 4388

[5] Ping D H, Hono K and Hirosawa S 1998 *J. Appl. Phys.* **83** 7769

[6] Yang B, Shen B G, Zhao T Y and Sun J R 2007 *Acta Phys. Sin.* **56** 3527 (in Chinese)

[7] Pang L J, Sun G F, Chen J F, Qiang W J, Zhang J B and Li W A 2006 *Acta Phys. Sin.* **55** 3049 (in Chinese)

[8] Gong W, Hadjipanayis G C and Krause R F 1994 *J. Appl. Phys.* **75** 6649

[9] McCormick P G, Miao W F, Smith P A I, Ding J and Street R 1998 *J. Appl. Phys.* **83** 6256

[10] Zhang J, Zhang S Y, Zhang H W, Shen B G and Li B H 2001 *J. Appl. Phys.* **89** 2857

[11] Shindo M, Ishizone M, Kato H, Miyazaki T and Sakuma A 1996 *J. Magn. Magn. Mater.* **161** L1

[12] Fullerton E E, Jiang J S, Sower C H, Pearson J H and Bader S D 1997 *Appl. Phys. Lett.* **72** 380

[13] Liu J P, Luo C P, Liu Y and Sellmyer D J 1998 *Appl. Phys. Lett.* **72** 483

[14] Zeng H, Li J, Liu J P, Wang Z L and Sun S 2002 *Nature* **420** 395

[15] Gao Y, Bao Y, Beerman M, Yashuhara A, Shindo D and Krishnan K M 2004 *Appl. Phys. Lett.* **84** 3361

[16] Hubert A and Schafer R 1998 *Magnetic Domains* (Berlin: Springer-Verlag)

[17] Fullerton E E, Jiang J S and Bader S D 1999 *J. Magn. Magn. Mater.* **200** 392

[18] Leineweber T and Kronmuller H 1997 *J. Magn. Magn. Mater.* **176** 145

[19] Gao Y, Shindo D and Petford-Long A K 2003 *J. Appl. Phys.* **93** 8119

[20] Kondorskij E 1940 *J. Phys. USSR* **2** 161